

Novel Control of FLAMI with Super Twisting Sliding Mode Controllers for Grid Connected PMSG based Wind Power Conversion System

Sushil Kumar Bhoi¹, Mihira Kumar Nath²

^{1,2}Department of Electrical Engineering, Government College of Engineering Kalahandi, State-Odisha, Country-India

Email: sushilkumarbhoi@gmail.com¹, mihirnath.83@gmail.com²

Received: 19.04.2024

Revised : 18.05.2024

Accepted: 24.05.2024

ABSTRACT

Electricity serves as a fundamental necessity in society, enabling the completion of numerous tasks. The generation of electric power from renewable energy sources (RESs) linked to the power grid is attracting significant interest from numerous researchers, owing to its potential to diminish pollution and its various benefits. Among various options, electric power generation using variable speed wind turbines has gained significant popularity and necessitates innovative control methodologies for effective integration with the power grid. Detecting the wind speed of a wind turbine poses challenges, particularly in high power applications. Therefore, a maximum power point tracking (MPPT) algorithm that does not rely on speed sensors has been developed to optimize power extraction from the wind turbine across a range of operating conditions. Permanent Magnet Synchronous Generators (PMSGs) are frequently employed in wind power conversion systems for the generation of electrical energy. Additional multilevel inverters are necessary for the integration of PMSG based wind power conversion systems into the power grid; however, they are challenged by an increased number of power electronic switches. Consequently, this paper examines a Five Level Aligned Multilevel Inverter (FLAMI). In contrast to traditional PI controllers, super twisting sliding mode (STSM) controllers demonstrate superior performance during rapid fluctuations. Consequently, this paper presents a new control methodology for a FLAMI designed for a grid-connected PMSG-based wind power conversion system. Furthermore, a whale optimization technique is employed to adjust the various parameters utilized in STSM controllers. A range of outcomes is analyzed through the Hardware-in-the-Loop setup implemented on the OPAL-RT platform.

Keywords: Super twisting sliding mode controller, Grid connected system, PMSG, Wind power conversion system, Whale optimization, Power Quality.

1. INTRODUCTION

Electrical power plays a crucial role in daily human activities, facilitating a wide range of tasks, and it significantly contributes to the development of any nation. The demand for electricity generation is rising steadily; however, traditional sources such as oil and coal are not only finite but also detrimental to the environment due to the emission of harmful gases into the atmosphere. Consequently, numerous sectors around the globe are seeking to employ REPS for electricity generation, particularly in WPCSs [1-2]. Furthermore, the use of WPCSs for electricity generation is highly recommended because of their various advantages, such as sustainability, lower greenhouse gas emissions, and the capacity to utilize a RES. These systems harness the kinetic energy produced by wind to generate electricity, positioning them as a sustainable alternative to fossil fuels. Furthermore, technological advancements have enhanced the efficiency and dependability of wind power systems, establishing them as a feasible choice for both extensive energy generation and smaller, localized uses. As nations endeavor to fulfill their energy requirements while tackling climate change, the implementation of WPCS is increasingly recognized as an essential measure for achieving a more sustainable energy future.

Overall, the adoption of WPCSs employing PMSG technology in grid-connected applications is on the rise, attributed to their various benefits. These systems capture the kinetic energy produced by wind and transform it into electrical energy, which can subsequently be integrated into the electrical grid. PMSG technology is highly preferred for a variety of reasons. To begin with, PMSGs are recognized for their exceptional efficiency and dependability, which are essential elements in optimizing energy production and maintaining stable performance across diverse wind conditions. In contrast to conventional induction

generators, PMSGs operate without the need for external excitation, thereby streamlining the design process and minimizing maintenance requirements. Additionally, PMSGs demonstrate outstanding efficiency at low wind speeds, rendering them appropriate for a broader spectrum of wind conditions. This feature enhances energy capture and improves the overall efficiency of wind farms. Furthermore, the compact configuration of PMSGs allows for greater flexibility in installation, which can be especially advantageous in locations where space is limited. In applications connected to the grid, WPCSs utilizing PMSG can seamlessly integrate with the current electrical infrastructure. They are capable of delivering not only energy but also supplementary services, including frequency regulation and voltage support, thereby improving the stability and reliability of the electrical grid. In addition, the capability to regulate output power via sophisticated power electronics enhances the management of energy flow, thereby fostering a more robust energy system. With the rising demand for REPS, the implementation of WPCSs that employ PMSG technology is anticipated to rise, significantly contributing to the shift towards sustainable energy solutions. This trend is bolstered by continuous technological advancements that seek to enhance the efficiency, cost-effectiveness, and overall performance of wind energy systems.

To achieve the highest possible energy extraction from wind turbines, it is essential to implement a MPPT circuit in conjunction with an effective algorithm [2-3]. Nevertheless, conventional MPPT methods necessitate the turbine's speed signal, which poses challenges in terms of maintenance and incurs higher costs in real-time applications. Occasionally, the sensors employed to measure turbine speed may experience malfunctions as a result of factors such as heat, dust, and prolonged operation. Therefore, it is essential to implement MPPT operation that does not rely on speed sensors. Consequently, a three-phase controllable rectifier utilizing SMC is implemented for the operation of MPPT, thereby removing the requirement for any speed signal from the turbine or PMSG. The suggested approach will provide the reference current component for the quadrature axis within the control methodology of the rectifier. Therefore, this rectifier is unable to control the dc-link voltage, which is the output of the rectifier. Consequently, the inverter employed to connect the dc-link to the power grid must control the voltage at the dc-link. Traditional inverters tend to introduce a greater amount of harmonics into the power grid, which is why multilevel inverters are preferred [4-5] must be used for high power applications. Nevertheless, conventional topologies of multilevel inverters are hindered by an excessive number of power electronic switches. Consequently, this paper employs a three-phase FLAMI system that necessitates only four switches for each phase [5]. A new control methodology has been developed for FLAMI, encompassing multiple objectives.

Typically, conventional PI controllers face challenges in producing accurate reference signals amid swift variations in the system. Consequently, the proposed control methodology employs STSM controllers to achieve a rapid and precise response across a range of operating conditions [6-8]. Nevertheless, numerous parameters must be estimated in different STSM controllers. Therefore, WOA [9] is utilized to achieve the optimized parameters for different STSM controllers. A five-level space vector modulation technique is utilized to achieve effective synchronization with the grid. Generally, loads function at the GCP, demonstrating characteristics of imbalance, nonlinearity, and reactive power. Consequently, these loads may negatively impact the quality of power, particularly when they are connected to the power grid. Consequently, the proposed control methodology also facilitates the regulation of voltage and the compensation of reactive power at the GCP, thereby improving the overall power quality of the system. The Hardware-in-the-Loop (HIL) testing is conducted utilizing OPAL-RT racks to showcase a range of results for further analysis. The specific objectives of this paper are outlined below:

- Execute the SMC-based MPPT for WPCSs.
- Create an innovative control technique for a FLAMI.
- In order to achieve the best possible responses across various operating conditions, the suggested control methods integrate STSM controllers.
- In order to illustrate the functionality of HIL, two OPAL-RT devices are utilized to present various results from several case studies.

Additionally, the paper is organized into the following sections. An overview of the entire system is provided in Section II. Section III outlines the proposed methodology for MPPT control of WPCS utilizing SMC. A comprehensive description of the proposed control methodology for the FLAMI, in conjunction with the STSM controller, is provided in Section IV. Section-V has been compressed using the WOA to optimize the parameters of STSM controllers. Section VI presents a range of results derived from HIL, which are subsequently analyzed. The conclusion can be found in Section VII.

2. Overview of Grid Connected PMSG based WPCS

Figure 1 illustrates a grid-connected PMSG based WPCS integrated with FLAMI. A gear mechanism is

employed to modify the rotational speed of the PMSG shaft [10]. A three-phase controllable rectifier is employed to convert the output of the PMSG into a direct current (DC) source. Additionally, it can function as a MPPT converter by incorporating the proposed control methodology of the MPPT algorithm. A two-mass wind drive train is examined based on the findings in [1]. The wind turbine model is constructed utilizing the methodologies outlined in [2-3]. References [10-12] are employed to model the PMSG, while the FLAMI is developed using the information from [5, 13]. The output voltage and frequency of PMSGs cannot remain constant, as they are influenced by variations in wind speed. Therefore, it is essential to implement an efficient control system for the three-phase rectifier that can regulate the current flowing into the DC link in accordance with the directives provided by the MPPT algorithm utilizing SMC. Although there are various algorithms available for optimizing the energy output of wind turbines, the SMC method stands out as one of the most effective options [14]. To prevent the use of multiple sensors, SMC is designed to operate solely based on the current and voltage present at the DC link. Therefore, wind turbines do not require speed sensors.

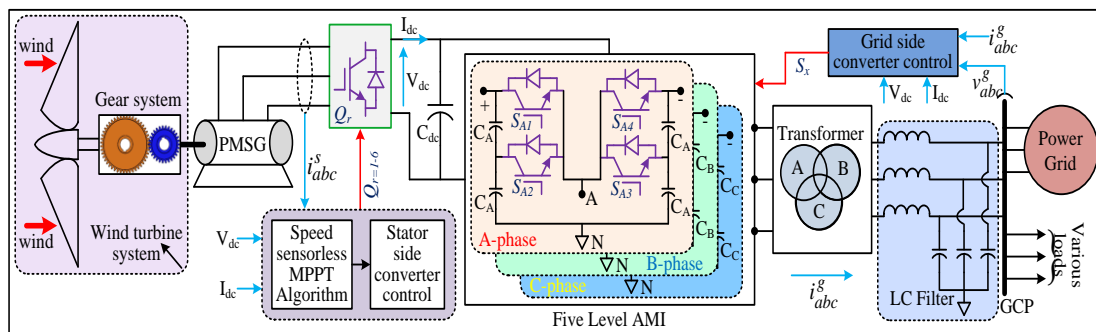


Figure 1. Grid connected PMSG based WPCS with FLAMI.

Numerous researchers have created systems of a comparable nature, with only a limited number of notable systems being emphasized in the literature review. The authors in [15] introduced a MPPT system for a grid-connected configuration utilizing PMSG and PV technology. The authors in [16] propose a new control method for WPCS that are connected to the grid and utilize PMSG in the context of unbalanced voltage conditions. The authors in references [17-18] present an H-bridge multilevel inverter designed for grid-connected PMSG based WPCS, specifically for STATCOM applications, utilizing a coordinated control strategy. The authors in [19] present a study on the modeling and control of WPCS that are connected to the grid and utilize PMSG. The authors in references [20-22] present a stability analysis utilizing various methodologies for grid-connected PMSG based WPCS. Nevertheless, the authors referenced in [15-22] have not included STSM controllers and speed sensorless-based SMC in their models. A range of parameters for the 5MW PMSG-based WPCS is presented in Table-1 [23].

Table 1. Parameters of PMSG-WPCS.

S.No	Parameter name	Value
1	Number of poles	8
2	Operating frequency (Hz)	50.0
3	Stator slots	24
4	Resistance of armature/phase	0.0375
5	Reactance of D-Q axis (Ohm)	2.93
6	Line to line RMS voltage (kV)	5.032
7	Line current (RMS) (A)	742.962
8	Armature current density(A/mm ²)	5.5
	Iron core and armature copper losses (kW)	9.883; 6.2061
	Rated Speed (rpm)	750
	Power factor	0.81
	Rated Power (MW)	5.0

3. Proposed MPPT of WPCS

Numerous authors have suggested and developed a range of algorithms aimed at optimizing the energy harvesting of WPCS by ensuring its operation at the MPPT point. Numerous algorithms necessitated the measurement of wind turbine speed using a variety of sensors. Nevertheless, it will pose greater

challenges, necessitating maintenance and replacements, and may be susceptible to malfunctions. Therefore, it is essential to implement speed sensorless MPPT algorithms. Consequently, this paper presents the development of a SMC that relies solely on the single measurements of current and voltage, specifically after the output of the PMSG. Hence, no need of signals from turbine side. This document outlines the advancement of SMC [16-17] utilizing a three-phase rectifier, which allows for the transfer of current from the PMSG side to the dc-link, thus facilitating the regulation of the shaft speed of the PMSG. The shaft of the PMSG is linked to the wind turbine through a gear mechanism, which facilitates the adjustment of the wind turbine's speed in alignment with its MPPT level. The output signal generated by the proposed SMC will subsequently be utilized as the input signal for the control methodology of the three-phase rectifier. The suggested control approach for MPPT, which is linked with SMC, employs STSM controllers. Therefore, the specifications of the STSM controller are presented prior to discussing the control method of the MPPT.

The STSM controller is a well-respected approach that has garnered significant recognition in relation to numerous nonlinear systems [7-8]. The STSM controller effectively addresses the chattering issues commonly associated with traditional sliding mode control, thus enabling more seamless control. The block diagram of the STSM control system is depicted in Figure 2. The modification of variables a_0 to a_3 poses considerable difficulties when utilizing multiple STSM controllers in the suggested control framework. As a result, this study utilizes the WOA process to identify the most effective combination of various parameters to achieve the desired outcomes under different operating conditions. The detailed process of the WOA is described in Section-V.

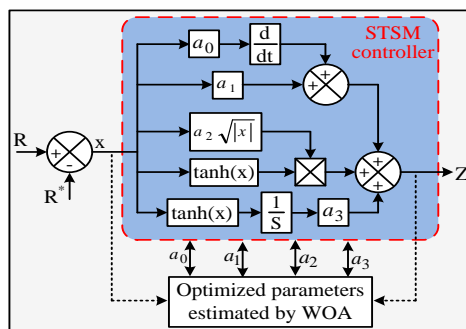


Figure 2. Generalized block of STSM controller.

To attain enhanced performance compared to traditional PI and Fuzzy controllers, the control methodology for the MPPT incorporates STSM controllers [18]. The control methodology proposed for the SMC linked to the MPPT of WPCS is illustrated in Figure 3. The SMC is producing a reference component for the present quadrature and is controlling the speed of the PMSG by adjusting the torque. The rotational speed of the PMSG shaft can be regulated, enabling the modification of the wind turbine's speed to attain optimal performance. The discrepancy between the actual and reference quadrature current is provided as input to the STSM controller-1. Similarly direct axis is assigned to STSM controller-2. To limit the power conversion from DC to AC, the reference signal for the direct axis component is established at a value of zero. The generated pulses are given to three phase rectifier. The parameters such as $\alpha, \beta, \delta, \rho$, among others, that are integral to SMC are adjusted using the particle swarm optimization technique. This method necessitates only the measurement of currents and voltages, without the need for any speed signal from the WPCS.

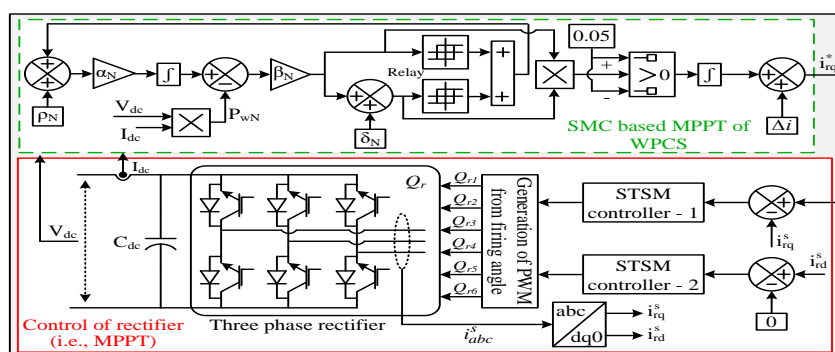


Figure 3. Proposed control methodology of three phase rectifier to work as a MPPT of WPCS.

4. Control Methodology of FLAMI

An inverter is required to be installed between the DC link and the power grid in order to convert and transfer DC power to the grid. This study employs a FLAMI in combination with the SVPWM technique to guarantee the delivery of high-quality power to the grid lines. It is crucial to develop an effective control strategy for the inverter to manage active power, mitigate reactive power, and respond to the effects of unbalanced loads. This inverter is necessary for the injection of currents into three-phase grid lines by controlling the voltages at both the DC link and the GCP. Numerous AC loads are functioning at the GCP, and these loads will introduce nonlinear currents that degrade the power quality of the power grid by generating harmonics. Therefore, the design of the proposed inverter control should be structured in a manner that enhances power quality by alleviating the impacts caused by local loads at the GCP. The control mechanism for the inverter is illustrated in Figure 4. The actual power produced by the PMSG can be transmitted into the power grid by ensuring that the voltage of the DC link remains at its designated reference value. The oscillating part of the V_{dc} is derived by utilizing a low pass filter (LPF), which is then compared to 'Zero' to reduce the effects of unbalanced loads within the dc-link. The objective of this process is to reduce the second frequency oscillations occurring on the shaft of the PMSG, which in turn improves the fatigue life of the shaft. The inverter's reactive current component is derived by assessing the RMS voltage against its reference, thereby enabling the necessary compensation for the reactive power at the GCP. The appropriate STSM controllers will generate the reference signals for the DQ-axis, which will act as inputs for the space vector pulse width modulation (SVPWM) method [4, 24]. A five-level SVPWM technique has been developed for FLAMI to generate the necessary output voltages. The decoupling components were also incorporated to eliminate the voltage drops across the LC filter. The inverters will perform functions akin to those of a DSTATCOM and an active power filter, aimed at compensating for reactive power, regulating the RMS voltage, and alleviating the impact of nonlinear loads on the grid lines. Additionally, the proposed method aids in attaining balanced grid currents despite the presence of unbalanced loads at the GCP by incorporating counter currents into the power grid lines.

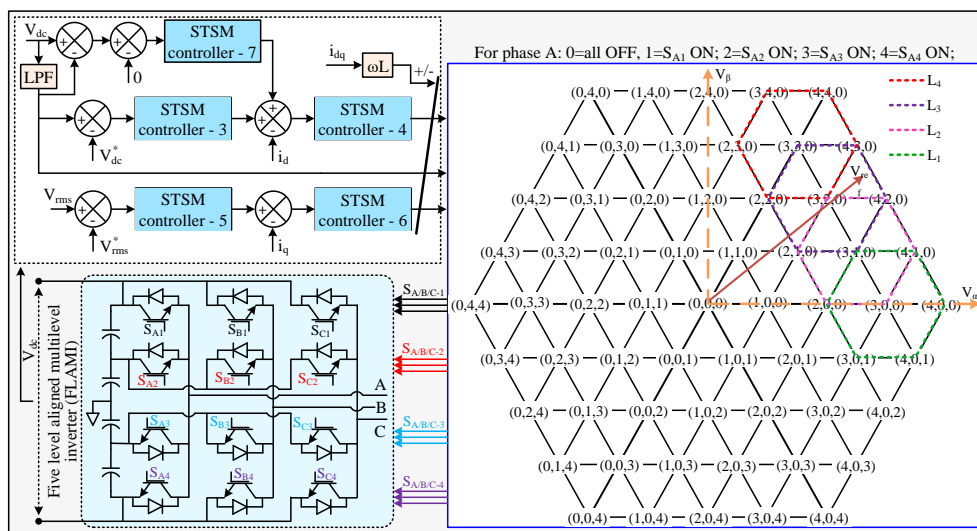


Figure 4. Control methodology of inverter.

5. WOA based STSM Controllers

The WOA enables the modification of multiple parameters of the STSM controllers to optimize their performance across different operating conditions. This procedure can be executed by employing the mathematical calculations specified in the provided equation. In 2016, Mirjalili and Lewis introduced the WOA algorithm [9], a meta-heuristic optimization technique designed to address nonlinear problems that involve multiple objective functions. Humpback whales demonstrate remarkable hunting abilities in comparison to other whale species, especially through their distinctive bubble-net feeding method. The foraging behavior encompasses the formation of unique bubbles that are organized in a spiral or linear pattern. The detailed procedure of WOA is discussed in the subsequent sections [9].

Section-A: WOA is acknowledged as a premier optimization method for determining the appropriate parameters in real-time to achieve the optimal solution. As mentioned earlier, Humpback whales are capable of utilizing a bubble net technique to encircle a particular school of fish in a circular arrangement while engaging in their hunting practices. The entire process can be elucidated by employing the following essential equations.

$$\bar{D} = \left| \bar{C} \bullet \bar{a}_i^{k*}(j) - \bar{a}_i^k(j) \right|; \quad i = 0,1,2,3 \text{ for } k^{\text{th}} \text{ STSM controller}$$

(1)

$$\bar{a}_i^k(j+1) = \bar{a}_i^{k*}(j) - \bar{A} \bullet \bar{D}$$

(2)

In this context, the character 'j' signifies the present iteration.

Section-B: The ideal location of the Whale concerning the parameter (ai) is represented by the position vector, as mentioned earlier. In applying the WOA technique, we drew inspiration from humpback whales, known for their distinctive behavior of surrounding their prey in a spiral formation. The mathematical depiction of this spiral shape can be expressed through the following equations.

$$\bar{D}' = \bar{a}_i^{k*}(j) - \bar{a}_i^k(j)$$

(3)

$$\bar{a}_i^k(j+1) = \begin{cases} \bar{a}_i^{k*}(j) - \bar{A} \bullet \bar{D} & \text{if } p < 0.5 \\ \bar{D}' \bullet e^{bl} \bullet \cos(2\pi l) + \bar{a}_i^{k*}(j) & \text{if } p \geq 0.5 \end{cases}$$

(4)

$$\bar{D} = \left| \bar{C} \bullet \bar{a}_{i \text{ rand}}^k - \bar{a}_i^k \right|$$

(5)

$$\bar{a}_i^k(j+1) = \bar{a}_{i \text{ rand}}^k - \bar{A} \bullet \bar{D}$$

(6)

Section-C: Once the WOA method identifies the most suitable search agents, the strategy will then modify the positions and paths of the remaining search agents in relation to their proximity to the leading agent. Furthermore, this iterative process will persist until it identifies the overall optimal solution. This procedure can be categorized into two separate approaches, which are detailed below:

Shrinking encircling mechanism: This approach aids in guiding whales to their desired location by minimizing the distance from their present position to the intended destination. From a mathematical standpoint, this approach entails reducing the present vector value by diminishing the variable, as demonstrated in the subsequent equations:

$$\bar{A} = 2\bar{d} \bullet \bar{r} - \bar{d}$$

(7)

$$\bar{C} = 2 \bullet \bar{r}$$

(8)

Spiral updating position: This method enables the alteration of whales' movement and path by evaluating the distance between the whale(s) and the prey or intended target area. This idea is primarily illustrated by the mathematical equation presented here.

$$\bar{a}_i^k(j+1) = \bar{D}' \bullet e^{bl} \bullet \cos(2\pi l) + \bar{a}_i^{k*}(j)$$

(9)

The above process will be continued until the error (input) of the STSM controller becomes very minimum.

6. RESULTS

The setup depicted in Figure 1 is executed on a real-time simulation platform utilizing OPAL-RT technologies. The HIL configuration consists of the integration of two OPAL-RT units [25]. One module functions as a system comprising WPCS, converters, the grid, loads, inductors, capacitors, and other components, whereas the other module is dedicated to developing the control methodologies, as illustrated in Figures 3 and 4. The setup of the HIL system is achieved through the transmission of analog signals from the OPAL RT1 module to the control unit module, referred to as OPAL RT2. In a similar manner, digital signals are conveyed from unit-2 to unit-1. To establish a HIL simulation, it is crucial to segment the system into two fundamental components: the Plant and the Controller. The plant is represented through 'OPAL-RT'1, while the controller block is represented using 'OPAL-RT'2. A variety of case studies have been conducted to assess the importance and validate the efficacy of the system. Several supplementary parameters of the system are obtained from [26-27]. Figure 5 shows the basic HIL setup.

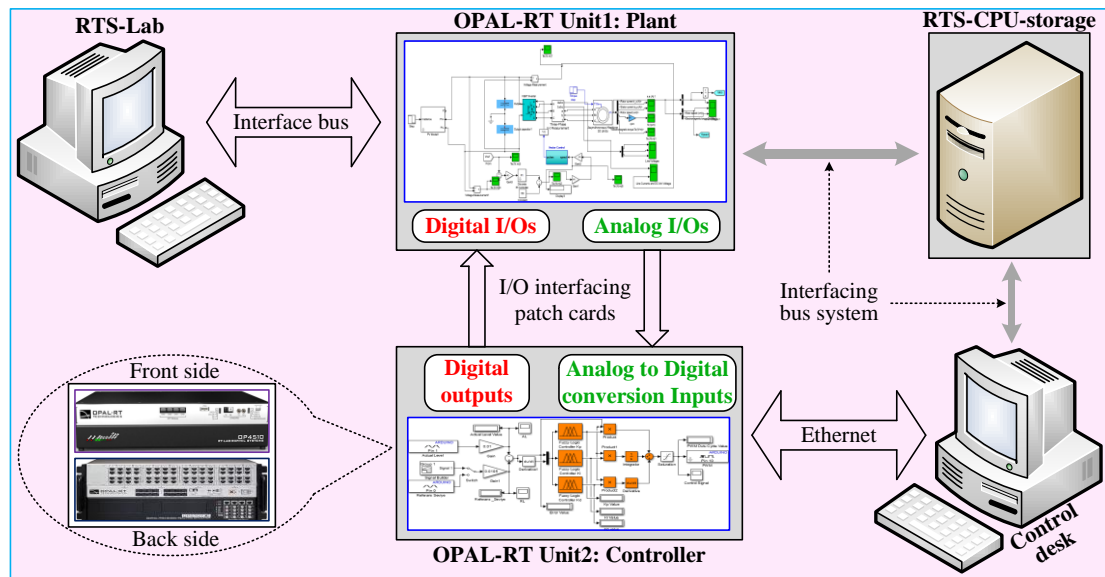


Fig 5. HIL setup with two OPAL-RT modules

Case-A: MPPT performance of WPCS

A dual-mass model of a wind turbine has been developed to enhance the accuracy of MPPT results. The model takes into account variations in wind speed, which decreases from 12.0 m/s to 7.0 m/s at $t = 2.0$ seconds, and subsequently rises from 7.0 m/s to 10.0 m/s at $t = 6.0$ seconds, as illustrated in Figure 6. During these transformations, the torque produced by the wind turbine consistently corresponds with the reference torque obtained from wind turbine data [1, 3]. The illustration provided in Figure 6 illustrates the features of both the reference torque and the mechanical torque in the wind turbine system. A sudden decline in wind speed, which is a characteristic aspect of the two-mass model, leads to a progressive reduction in torque. As demonstrated in Figure 6, the wind turbine system operates at its peak power output [1, 3]. The alignment of the torque produced by the PMSG associated with the turbine to the reference torque is achieved through the current regulation of the three-phase rectifier.

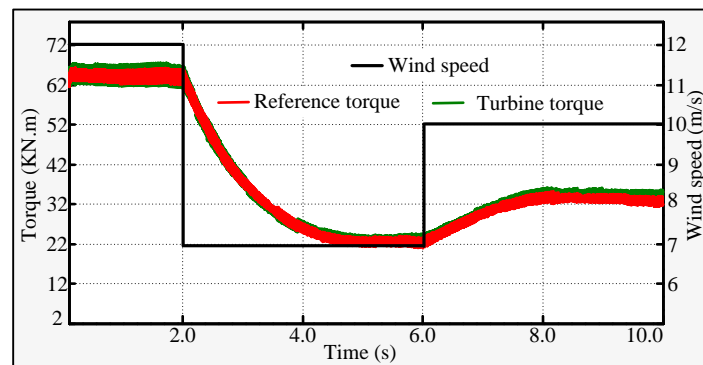


Figure 6. MPPT action of WPCS with SMC and STSM controllers.

Case-B: Operation with unbalanced loads

Figure 7(a) depicts the unbalanced currents that arise from a three-phase load at the GCP. The presence of an unbalanced load at the GCP necessitates the power grid to supply unbalanced currents, resulting in the generation of unbalanced grid currents due to inconsistent voltage drops along the transmission lines. Consequently, the suggested inverter control will operate to generate counter-phase currents and inject them into the GCP, thereby facilitating a balance in the currents of the power grid lines. Figure 7(b) depicts the balanced currents within the grid. In the absence of power supply from the WPCS, the inverter functions as an interline power flow controller, ensuring that the currents within the power grid remain balanced. Figure 7(c) illustrates the balance of the corresponding voltages at the GCP. In this particular case study, an analysis of an unbalanced load was conducted at $t = 2.0$ seconds. The oscillations generated in the WPCS due to the unbalanced load are depicted in Figure 7(d). This analysis involves a comparison of the conventional control strategies of the inverter with the proposed control strategies, focusing on the

currents. The application of the suggested control leads to diminished oscillations, consequently improving the fatigue lifespan of the shaft.

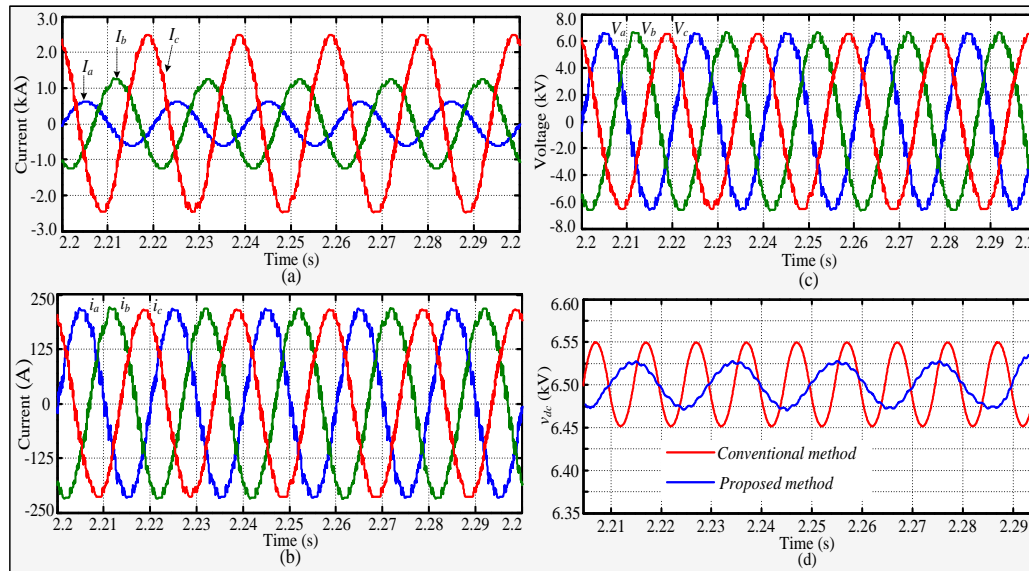


Figure 7. Responses of (a) unbalanced load currents, (b) balanced currents of grid lines, (c) voltages at GCP, and (d) oscillations in dc-link.

The controller being evaluated is additionally subjected to testing with nonlinear loads. Figure 8 presents the total harmonic distortion (THD) obtained from the fast Fourier transform (FFT) analysis of the phase voltage.

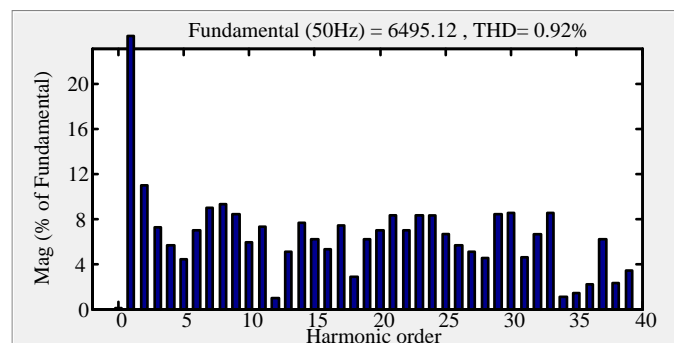


Figure 8. THD Analysis.

Case-C: Performance of WOA

The error signal response from V_{rms} is taken into account for the purpose of comparing the proposed methods: WOA, PSO (particle swarm optimization), MGWO (modified grey wolf optimization), and MIWO (modified invasive weed optimization). A significant alteration of 75% load is implemented at $t=7.50$ seconds at the GCP for the purpose of testing in this scenario. The various parameters of the STSM controllers utilized in the proposed method are derived from PSO, MGWO, MIWO, and WOA. Using these parameters, the error signal response (as a percentage of the normalized value from the equation below) is shown in Figure 9. An examination of Figure 9 reveals that the response has enhanced through the application of the proposed method utilizing WOA. The error remains minimal when optimized parameters are employed with WOA.

$$\% \text{ of normalized } V_{rms} = \frac{V_{rms}^* - V_{rms}}{V_{rms}^*} \times 100 \tag{10}$$

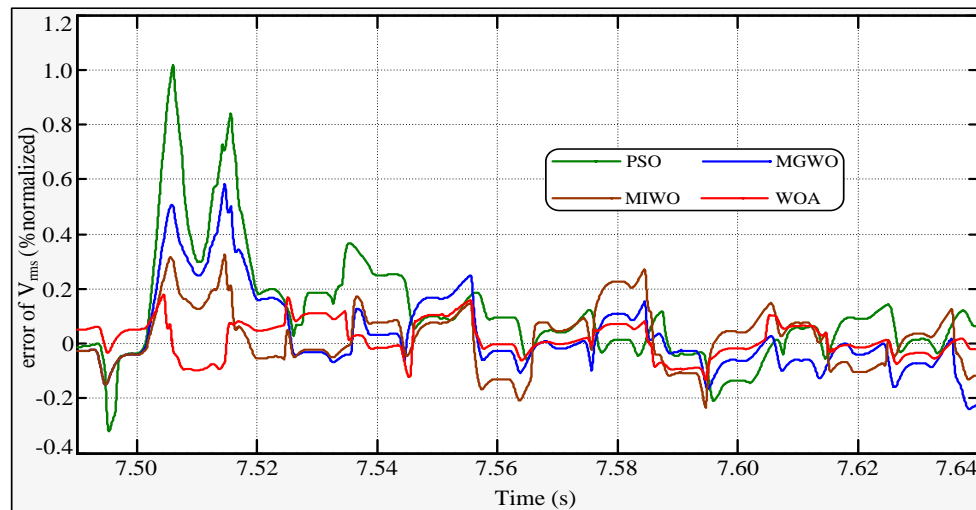


Figure 9. Response of error signal with PSO, MIWO, MGWO and WOA.

7. CONCLUSION

This document introduced a comprehensive control strategy developed for grid-connected PMSG based WPCS, with the objective of improving the quality of power delivered at the GCP. Control strategies utilizing SMC have been applied for MPPT in WPCS through the use of three-phase controllable rectifiers managed by STSM. The proposed control strategy is designed to enhance the injection of active power into the power grid, address reactive power compensation, and manage unbalanced loads, while also mitigating the effects of nonlinear loads. The results obtained from OPAL-RT demonstrate the efficacy of this approach and emphasize the potential of the STSM-based controller in managing PMSG-based grid-connected WPCS utilizing a Real-Time Simulator. A HIL configuration has been established to facilitate a more authentic simulation and evaluation of the controller.

REFERENCES

- [1] Bhoi, S.K., Meher, B. and Panigrahi, J.K., 2024. Novel Control of PV-Battery Powered Standalone Power Supply System with Neuro-Fuzzy Controller. *Revista Electronica de Veterinaria*, 25(1), pp.733-740.
- [2] Shill, K., 2024. A Hybrid System Combining Photovoltaic, Wind Turbine, Diesel Generator, and Battery Storage Technologies. *J. Electrical Systems*, 20(3), pp.2969-2984.
- [3] Bhoi, S.K., Shill, P.K., Behera, N., Baliarsingh, A.K. and Bagal, D.K., 2024. Voltage Control of PV-Wind-FCElectrolyzer-Battery based Hybrid Microgrid. *Journal of Electrical Systems*, 20(2), pp.2679-2695.
- [4] P. K. Chamarthi, U. R. Muduli, M. S. E. Moursi, A. Al-Durra, A. S. Al-Sumaiti and K. Al Hosani, "Improved PWM Approach for Cascaded Five-Level NPC H-Bridge Configurations in Multilevel Inverter," in *IEEE Transactions on Industry Applications*, doi: 10.1109/TIA.2024.3409511.
- [5] Name-Azra Zaineb, et. al., "Fuzzy Controller based Closed Loop Control for Single Stage Single Phase Grid Integrated PV System with Novel Configuration of 7 Level Hybrid Inverter", *E3S Web of Conf 1st International Conference on Power and Energy Systems (ICPES 2023)*, Volume 540, June 2024, <https://doi.org/10.1051/e3sconf/202454010004>.
- [6] Z. Li, S. Zhou, Y. Xiao and L. Wang, "Sensorless Vector Control of Permanent Magnet Synchronous Linear Motor Based on Self-Adaptive Super-Twisting Sliding Mode Controller," in *IEEE Access*, vol. 7, pp. 44998-45011, 2019, doi: 10.1109/ACCESS.2019.2909308.
- [7] P. Gao, G. Zhang, H. Ouyang and L. Mei, "An Adaptive Super Twisting Nonlinear Fractional Order PID Sliding Mode Control of Permanent Magnet Synchronous Motor Speed Regulation System Based on Extended State Observer," in *IEEE Access*, vol. 8, pp. 53498-53510, 2020, doi: 10.1109/ACCESS.2020.2980390.
- [8] J. Zhai and Z. Li, "Fast-Exponential Sliding Mode Control of Robotic Manipulator With Super-Twisting Method," in *IEEE Transactions on Circuits and Systems II: Express Briefs*, vol. 69, no. 2, pp. 489-493, Feb. 2022, doi: 10.1109/TCSII.2021.3081147.
- [9] N. Katta, M. P. Kumar, K. Mahender, D. N. Santoshi Rupa Priyanka Malla and S. G. Malla, "Whale Optimization based MPPT of Single Stage Grid Connected PV System with H_{∞} Controller," *2022 1st IEEE International Conference on Industrial Electronics: Developments & Applications (ICIDeA)*, Bhubaneswar, India, 2022, pp. 220-226, doi: 10.1109/ICIDeA53933.2022.9970020.

- [10] A. D. Lilla, H. Dehnavifard, M. A. Khan and P. Barendse, "Optimization of high voltage geared permanent-magnet synchronous generator systems," 2014 International Conference on Electrical Machines (ICEM), Berlin, Germany, 2014, pp. 1356-1362, doi: 10.1109/ICELMACH.2014.6960358.
- [11] P. Kumar, D. V. Bhaskar, R. K. Behera and U. R. Muduli, "Continuous Fast Terminal Sliding Surface-Based Sensorless Speed Control of PMSBLDCM Drive," in *IEEE Transactions on Industrial Electronics*, vol. 70, no. 10, pp. 9786-9798, Oct. 2023, doi: 10.1109/TIE.2022.3225850.
- [12] S. S. Samal, B. K. Panigrahi, S. Mohapatra, A. Barpanda, V. Das and M. K. Das, "Modeling and Control of PMSG Based Wind Energy Generation System," 2019 International Conference on Intelligent Computing and Control Systems (ICCS), Madurai, India, 2019, pp. 571-575, doi: 10.1109/ICCS45141.2019.9065852.
- [13] Nagaraju, Motaparathi and Malligunta, Kiran Kumar. "Grid integration of hybrid renewable energy source using Aligned Multilevel Inverter" *International Journal of Emerging Electric Power Systems*, vol. 23, no. 5, 2022, pp. 691-702. <https://doi.org/10.1515/ijeeps-2021-0366>.
- [14] B. Sarsembayev, K. Suleimenov, B. Mirzagalikova and T. D. Do, "SDRE-Based Integral Sliding Mode Control for Wind Energy Conversion Systems," in *IEEE Access*, vol. 8, pp. 51100-51113, 2020, doi: 10.1109/ACCESS.2020.2980239.
- [15] M. M. R. Singaravel and S. A. Daniel, "MPPT With Single DC-DC Converter and Inverter for Grid-Connected Hybrid Wind-Driven PMSG-PV System," in *IEEE Transactions on Industrial Electronics*, vol. 62, no. 8, pp. 4849-4857, Aug. 2015, doi: 10.1109/TIE.2015.2399277.
- [16] J. Liu, C. Zhao and Z. Xie, "Power and Current Limiting Control of Wind Turbines Based on PMSG Under Unbalanced Grid Voltage," in *IEEE Access*, vol. 9, pp. 9873-9883, 2021, doi: 10.1109/ACCESS.2021.3049839.
- [17] Y. Peng et al., "Coordinated Control Strategy of PMSG and Cascaded H-Bridge STATCOM in Dispersed Wind Farm for Suppressing Unbalanced Grid Voltage," in *IEEE Transactions on Sustainable Energy*, vol. 12, no. 1, pp. 349-359, Jan. 2021, doi: 10.1109/TSTE.2020.2995457.
- [18] M. K. K. Prince et al., "Coordinated Control of Grid-Connected PMSG Based Wind Energy System With STATCOM and Supercapacitor Energy Storage," in *IEEE Transactions on Industry Applications*, vol. 60, no. 3, pp. 5108-5118, May-June 2024, doi: 10.1109/TIA.2024.3371407.
- [19] M. K. K. Prince, M. T. Arif, A. Gargoom, A. M. T. Oo and M. E. Haque, "Modeling, Parameter Measurement, and Control of PMSG-based Grid-connected Wind Energy Conversion System," in *Journal of Modern Power Systems and Clean Energy*, vol. 9, no. 5, pp. 1054-1065, September 2021, doi: 10.35833/MPCE.2020.000601.
- [20] W. Du, Y. Wang, Y. Wang, H. F. Wang and X. Xiao, "Analytical Examination of Oscillatory Stability of a Grid-Connected PMSG Wind Farm Based on the Block Diagram Model," in *IEEE Transactions on Power Systems*, vol. 36, no. 6, pp. 5670-5683, Nov. 2021, doi: 10.1109/TPWRS.2021.3077121.
- [21] W. Du, Y. Wang, H. F. Wang, B. Ren and X. Xiao, "Small-Disturbance Stability Limit of a Grid-Connected Wind Farm With PMSGs in the Timescale of DC Voltage Dynamics," in *IEEE Transactions on Power Systems*, vol. 36, no. 3, pp. 2366-2379, May 2021, doi: 10.1109/TPWRS.2020.3031351.
- [22] W. Du, W. Dong and H. F. Wang, "Small-Signal Stability Limit of a Grid-Connected PMSG Wind Farm Dominated by the Dynamics of PLLs," in *IEEE Transactions on Power Systems*, vol. 35, no. 3, pp. 2093-2107, May 2020, doi: 10.1109/TPWRS.2019.2946647.
- [23] P. Roshanfekar, T. Thiringer, S. Lundmark and M. Alatalo, "Selecting IGBT module for a high voltage 5 MW wind turbine PMSG-equipped generating system," 2012 IEEE Power Electronics and Machines in Wind Applications, Denver, CO, USA, 2012, pp. 1-6, doi: 10.1109/PEMWA.2012.6316407.
- [24] Q. Zhao, N. Diao, X. Sun, C. Song, X. Zhao and Y. Wang, "SVPWM for Five-Level Active Neutral-Point-Clamped Converter Based on Multispace Voltage Vector Mapping and Midpoint-Voltage Self-Balancing Strategy," in *IEEE Transactions on Power Electronics*, vol. 37, no. 11, pp. 13456-13467, Nov. 2022, doi: 10.1109/TPEL.2022.3186169.
- [25] Bhoi, S.K., Baliarsingh, A.K. and Panigrahi, J.K., 2024. Smart Impedance and Grid Forming Converter Supported d-STATCOM. *Nanotechnology Perceptions*, pp.1293-1305.
- [26] C. N. Bhende, S. Mishra and S. G. Malla, "Permanent Magnet Synchronous Generator-Based Standalone Wind Energy Supply System," in *IEEE Transactions on Sustainable Energy*, vol. 2, no. 4, pp. 361-373, Oct. 2011, doi: 10.1109/TSTE.2011.2159253.
- [27] A. Radwan, M. A. Elshenawy, Y. A. -R. I. Mohamed and E. F. El-Saadany, "Grid-Forming Voltage-Source Inverter for Hybrid Wind-Solar Systems Interfacing Weak Grids," in *IEEE Open Journal of Power Electronics*, vol. 5, pp. 956-975, 2024, doi: 10.1109/OJPEL.2024.3410908.